

Published in final edited form as:

*J Immunol.* 2012 April 15; 188(8): 3920–3927. doi:10.4049/jimmunol.1102587.

## A deficiency in nucleoside salvage impairs murine lymphocyte development, homeostasis and survival<sup>1</sup>

Onjee Choi<sup>\*</sup>, Dean A. Heathcote<sup>\*,1</sup>, Ka-Kei Ho<sup>†,1</sup>, Phillip J. Müller<sup>\*</sup>, Hazim Ghani<sup>\*</sup>, Eric W.-F. Lam<sup>†</sup>, Philip G. Ashton-Rickardt<sup>\*</sup>, and Sophie Rutschmann<sup>\*</sup>

<sup>\*</sup>Section of Immunobiology, Faculty of Medicine, Imperial College London, Du Cane Road, London W12 0NN, UK

<sup>†</sup>Department of Surgery and Cancer, Faculty of Medicine, Imperial College London, Du Cane Road, London W12 0NN, UK

### Abstract

The homeostasis of the immune system is tightly controlled by both cell-extrinsic and –intrinsic mechanisms. These regulators, not all known to date, drive cells in and out of quiescence when and where required to allow the immune system to function. Here we describe a deficiency in deoxycytidine kinase (DCK), one of the major enzymes of the nucleoside salvage pathway, which affects peripheral T-cell homeostatic proliferation and survival. As a result of an N-ethyl-N-nitrosoUrea-induced mutation in the last  $\alpha$ -helix of DCK, a functionally null protein has been generated in the mouse and affects the composition of the hematopoietic system. Both B- and T-lymphocyte development is impaired, leading to a state of chronic lymphopenia and to a significant increase in the number of myeloid cells and erythrocytes. In the periphery, we found that mutant lymphocytes adopt a CD44<sup>high</sup>CD62L<sup>low</sup> memory phenotype, with high levels of proliferation and apoptosis. These phenotypes are notably the result of a cell-extrinsic driven lymphopenia-induced proliferation as wild-type cells transferred into DCK-deficient recipients adopt the same profile. In addition, DCK also regulates lymphocyte quiescence in a cell-intrinsic manner. These data establish *dCK* as a new regulator of hematopoietic integrity and lymphocyte quiescence and survival.

### Introduction

Throughout development and adult life, the immune system relies on homeostatic mechanisms to adjust to the many challenges it faces to maintain itself but also to respond to self and pathogenic antigens. In healthy unchallenged individuals, the rate of peripheral homeostatic proliferation remains low and hematopoietic cells are quiescent, conserving metabolic resources to survive for long periods of time, but also preventing from accumulating malignant metabolic and/or genetic damages(1). This quiescence of hematopoietic cells is actively positively and negatively maintained by both cell-intrinsic and -extrinsic factors, such as Forkhead box transcription factors, Tob and cytokines (IL-2, -7 and -15)(1-5). Genetic deficiencies in these regulators can result in severe human syndromes, ranging from acute and chronic leukemia, to several myeloproliferative diseases(3, 5, 6). However, not all the mechanisms controlling hematopoietic homeostasis

<sup>1</sup>The work was supported by a UK Medical Research Council grant to S.R. and P.G.A.R., a Cancer Research UK grant to P.G.A.R. and an Imperial College Elsie Widdowson award to S.R.

Correspondence: Sophie Rutschmann Tel: (44) 20 8383 1604 Fax: (44) 20 8383 2788 s.rutschmann@imperial.ac.uk.

<sup>1</sup>These authors contributed equally to this work.

The authors have no conflicting financial interests.

are known to date, and large numbers of patients are likely to harbor different genetic defects(6). In the course of an immune response, the activation of resting naïve T-cells by antigen presenting cells will drive them out of their quiescent state to undergo a massive phase of cellular proliferation(7). Once the antigen is cleared from the host, most of these T-cells will die to maintain the homeostasis of the T-cell pool. Few antigen-specific T-cells will survive and re-enter quiescence to prevent replicative senescence. These memory cells will remain in the host for long periods of time and provide a rapid and efficient protection to secondary infections. These events have been well described in the context of CD8<sup>+</sup> T-cell immune response to viral infections, which therefore provides a good model to identify new regulators of hematopoietic homeostasis.

In the cell, purine and pyrimidine nucleotides are synthesized by both *de novo* and salvage pathways that generate nucleotides from ribonucleoside diphosphate and deoxynucleoside, respectively(8). The salvage pathway is notably composed of four enzymes with overlapping specificities for the four native DNA precursors. These control the rate limiting phosphorylation of deoxynucleoside step : deoxycytidine kinase (dCK) and thymidine kinase 1 (TK1) in the cytosol, and mitochondrial thymidine kinase 2 (TK2) and deoxyguanosine kinase (dGK)(9). In particular, DCK directly phosphorylates deoxyadenosine, deoxycytidine and deoxyguanosine. Additional enzymes are also involved, as for example hypoxanthine phosphoribosyl transferase (HPRT) or adenosine deaminase (ADA). Deficiencies in purine and pyrimidine salvage have been associated with several human syndromes with many different symptoms(10). These include the neurological disease Lesch-Nyhan syndrome, due to HPRT deficiency and the immunological defect SCID, due to deficiency of either ADA or Purine Nucleoside Phosphorylase (PNP)(11-13). Deficiencies in dGK and TK2 result in mitochondrial DNA-depletion with fatal outcomes in both humans and mice(14-16). Mice deficient for TK1 develop kidney disease whereas those deficient for dCK display altered lymphocyte development(17, 18). In humans, a reduction in DCK enzymatic activity has been associated with resistance to antiviral and anticancer chemotherapeutic agents, whereas increased DCK enzymatic activity is associated with increased activation of these compounds to cytotoxic nucleoside triphosphate derivatives(19-21).

Here we report a null murine dCK mutant strain, *memi* (for memory interleukin-7 receptor phenotype) which presents, in addition to lymphocyte developmental deficiencies, changes in peripheral hematopoietic populations and a very high rate of cellular proliferation associated with an increased level of cell-death in peripheral lymphocytes. Our data indicate that this increased proliferation is due to both cell-extrinsic and –intrinsic effects. Our mouse model therefore supports an unexpected non-redundant role for dCK in homeostasis and survival of immune cells.

## Material and Methods

### Mice, mutagenesis and LCMV infection

The *memi* mutant mice were generated in a C57BL/6J background (C57BL/6J, Thy1.1 and 129SvImJ purchased from Charles River, France) and bred in Central Biomedical Services (Imperial College London, UK). Mice were kept under specific pathogen free conditions in individually ventilated cages. All animal procedures have been authorized in a British Home Office Animals Act License (PPL:70/6490). The ENU mutagenesis was performed as previously described(22). For the infection, mice were injected intraperitoneally with  $2 \times 10^5$  pfu LCMV Armstrong. At days 8 and 21 after the injection, lateral vein blood was analyzed by flow cytometry.

## Cell preparation and flow cytometry

Spleen and blood cells were incubated 5 minutes at room temperature in a RBC lysis buffer (0.85% (w/v)  $\text{NH}_4\text{Cl}$ , 50mM Tris, pH 7.2). All antibodies were from eBioscience (UK) except CD8 and TCRV $\beta$ 8 (BD bioscience, UK). LCMV-specific cells were detected with a PE-conjugated gp33-iTA $\beta$  MHC-I tetramer (Beckman Coulter, USA). The analysis of apoptosis was performed with anannexinV/PI kit (BD bioscience, UK). For proliferation and cell-cycle, a Ki-67 or an anti-BrdU antibody/7-AADkits were used (BD bioscience, UK). For BrdU experiments, mice were given freshly prepared 0.8mg/ml of BrdU (Sigma, UK) in drinking water daily for 5d. Samples were acquired on a DAKO Cyan 9 flow cytometer and data analyzed with the Summit<sup>TM</sup> software.

## dCK sequencing

The 7dCK exons were amplified from genomic DNA by PCR using the JumpStart REDTaq ReadyMix (Sigma, UK). PCR samples were purified by Qiagen PCR purification kit (Qiagen, UK), sequenced (Genomic laboratory, Imperial College, UK) and the data analyzed with the Sequencher software (Gene Codes Corporation, USA). The settings were: initialization 2 minutes/94C, denaturation 30 seconds/94C, annealing 30 seconds/60C, extension 90 seconds/72C.

Primers: exon1 (CGAGATTGACGCTGCAACC/AAGGGTGCACACTGGTCCAG), exon2 (GATGATGGTTGGTTATAGTTTGC/GCAGCTGTAGCTGGTTAGGAG), exon3 (AGCAACGTAGTGAGACCTTATC/CGCAGCCTCTAATTTGATTACC), exon4 (TGTTTGAAGGATGTCCATGC/TTTCAACAACACAGGCAAATG), exon5 (ACGGCAGCAGACACAACACTAG/ACAGTGAGCAGCAACCAGC), exon6 (GCATCACTACGGATGACGTTAG/TGTCCTGGACAAGACAAGACAC), exon7 (GGTTATTCAACCTACTACTGAAATACTTAG/CCACTCACTGCCCTGATGC).

## CD4<sup>+</sup> T-cell transfer and BM chimera

Splenic CD4<sup>+</sup> T-cells from *Thy1.2;dCK<sup>mem/mem</sup>* or *Thy1.1;dCK<sup>+/+</sup>* congenic mice were purified with magnetic beads (Miltenyi Biotec, UK). Three to 5 million cells from those donor groups were injected intravenously to non-irradiated *Thy1.2;dCK<sup>mem/mem</sup>* or *Thy1.1;dCK<sup>+/+</sup>* recipients. For bone marrow (BM) chimera, *Thy1.1;dCK<sup>+/+</sup>* wt recipients were fed antibiotics in the drinking water for 2 days and subsequently lethally irradiated with 900 rads. BM cells from either *Thy1.1;dCK<sup>+/+</sup>* wt or *Thy1.2;dCK<sup>mem/mem</sup>* mice were obtained and mature T-cells removed with Pan-T-cells magnetic beads (Miltenyi Biotec, UK). The BM cells were then mixed at a 1:1 ratio and  $10^6$  injected i.v. into each recipient mice. These were analyzed 5 weeks after injection.

## dCK kinase activity assay

Proteins were extracted by M-PER Mammalian Protein Extraction Reagent (Pierce, UK). Protein lysate (5 $\mu$ g) was incubated in DCK buffer (50mM Tris-HCL (pH 7.6); 5 mM UTP; 5 mM  $\text{MgCl}_2$ ; 2 mM DTT; 10 mM NaF; 1mM Thymidine), and the addition of 1 $\mu$ Ci 3H-CdA in final volume of 10 $\mu$ l. Reactions were carried out at 37C for 20 minutes, quenched with 40 $\mu$ l ice-cold water and heated at 90C for two minutes. The reactions were aspirated onto a wallac filter mat (Tomtec harvester 9600; Tomtec, USA and Wallac 1450-421; PerkinElmer, UK), washed three times in PBS, three times in 200 ml of 4 mM ammonium formate and twice for 2 minutes in 95% ethanol. The filter mat was placed at 60C for 10 minutes prior to addition of scintillation fluid. Enzyme kinetic properties were calculated by linear regression analysis using Michaelis–Menten plots.

## SDS PAGE and Western blot

Twenty  $\mu\text{g}$  of spleen proteins were size fractionized by SDS-PAGE and electrophoretically transferred onto nitrocellulose membrane (GE Healthcare, UK)(23). The primary antibodies used are: cyclin A (C-19), cyclin D3 (18B6-10), p27Kip1 (C-19), pRB (C-15) (Santa Cruz, USA), actin (ABcam, UK), Foxo3a (Millipore) and p32-Foxo3a (Cell Signalling). Secondary antibodies: rabbit anti-goat (SouthernBiotech, USA), goat anti-rabbit and goat anti-mouse (Dako, UK).

## Statistical analysis

All results are given as mean values with standard deviation (SD). Nonparametric unpaired t-test (two-tailed) was applied: \* $p < 0.05$ , \*\* $p < 0.01$ , \*\*\* $p < 0.001$ . All statistic calculations were performed with the Prism5 software (Graphpad, USA).

## Results

### The ENU-induced mutation *memi* impairs the immune response to viral infection

To identify new regulators of immune homeostasis, we have undertaken a germline mutagenesis and used the  $\text{CD8}^+$  T-cell response to lymphocytic choriomeningitis virus (LCMV) infection as a model to screen individual mutant mice. To this end, we have generated a library of third generation N-ethyl-N-nitrosoUrea (ENU) induced germline mutants in a pure C57BL/6J background. A total of 1480 individual mice were screened for modifications of immune responsiveness to LCMV. Their  $\text{CD8}^+$  response was assessed by measuring the percentage of antigen-specific CTL ( $\text{gp33}^+\text{CD8}^+$ ) and of effectors and memory precursors in the blood at the peak of expansion (d8 after infection) and at the end of contraction (d21). Four independent germline transmissible mutations which modify responsiveness to LCMV were isolated, of which a purely recessive one: *memi* was bred to homozygosity. Following LCMV infection, homozygous *memi* mutants mount an antigen-specific  $\text{CD8}^+$  T-cell response which is highly variable between individuals (Fig.1A). The antigen-specific population in *memi* mice is significantly enriched in effector cells ( $\text{KLRG1}^+\text{IL-7R}^-\text{gp33}^+\text{CD8}^+$ ) and deprived of memory precursors ( $\text{KLRG1}^-\text{IL-7R}^+\text{gp33}^+\text{CD8}^+$ ) (Fig.1B)(24). In addition, uninfected (naive) *memi* mutants are characterized by a dramatic decrease in  $\text{CD4}^+$  and  $\text{B220}^+$  lymphocytes, and a significant increase in cells of myeloid origin in the blood (Fig.1C). These data indicate that the *memi* mutation affects a gene essential for a qualitatively and quantitatively normal  $\text{CD8}^+$  T-cell immune response to LCMV infection, and for a normal hematopoietic composition in the blood.

### *memi* is a null mutation in deoxycytidine kinase (*dCK*)

To identify the causative *memi* mutation, we used a meiotic positional cloning strategy(25). Mice carrying the *memi* mutation were crossed to the 129SvImJ strain to obtain first generation hybrids which when intercrossed generated 21 second generation hybrids. These 42 meiotic events were analyzed for the linkage between 358 single nucleotide polymorphisms and the deficiency in  $\text{CD4}^+$  and  $\text{B220}^+$  blood lymphocytes, mapping the *memi* mutation to a 13.8Mb region on chromosome 5 with a logarithm of odds score of 5 (data not shown). This region contains 112 genes and pseudogenes (ensembl version 37.2), notably *dCK* encoding deoxycytidine kinase (DCK) which was considered a strong candidate based on the T-cell phenotype described for the knock-out mutant (*dCK*<sup>-/-</sup>)(18). Sequencing of *dCK* at the genomic DNA level in *memi* mice revealed a single nucleotide transversion (G to T) at nucleotide 739 (Fig.2A). This modification changes the glutamic acid 247 into an early translational terminating codon, removing the last 14aa of DCK.

To define the nature of the *memi* mutation, we measured DCK specific enzymatic activity in *dCK<sup>mem/mem</sup>*, *dCK<sup>mem/+</sup>* and *dCK<sup>+/+</sup>* wt mice. As negative and positive controls, we used *dCK*-deficient cells (L1210-10K) and their parental mouse lymphocytic leukemia line L1210, respectively (Fig.2B)(26). The L1210-10K *dCK*-deficient cell line was generated by growing L1210 leukemic cells in the presence of increasing concentration of gemcitabine. We found that the specific DCK enzymatic activity in *dCK<sup>mem/mem</sup>* splenocytes was reduced to the background levels observed in L1210-10K cells. This reduction in functionality was not due to an effect of the mutation on the mRNA or protein expression as both are produced normally in *dCK<sup>mem/mem</sup>* cells (Supp.Fig1). These data indicate that our point mutation abolishes DCK functional activity in homozygous mice to levels found in *dCK*-deficient cells, establishing our point mutation *dCK<sup>mem/mem</sup>* as a new recessive null allele of *dCK*.

### B- and T-lymphocyte development defects in *dCK<sup>mem/mem</sup>* mice

The analysis of *dCK<sup>-/-</sup>* mice implicated a role for the kinase in T- and B-cell development(18). The analysis of B-cell development showed a significant increase in the pro-B cells fractions A-C, correlating with a significant decrease in the pre-B cell fraction D (Supp.Fig.2).

*dCK<sup>mem/mem</sup>* thymuses were found to be reduced in size and cellularity (Fig.3A). In the thymus, T-cell precursors develop via the following chronological stages: double negative 1 (DN1, CD4<sup>-</sup>CD8<sup>-</sup>CD44<sup>+</sup>CD25<sup>-</sup>), DN2 (CD44<sup>+</sup>CD25<sup>+</sup>), DN3 (CD44<sup>-</sup>CD25<sup>+</sup>), DN4 (CD44<sup>-</sup>CD25<sup>-</sup>), double positive (DP, CD4<sup>+</sup>CD8<sup>+</sup>) and, finally, single positive (SP, CD4<sup>+</sup> or CD8<sup>+</sup>). In *dCK<sup>mem/mem</sup>* thymus, we observed a developmental blockage between the DN3 and the DN4 stages (Fig.3B). Proliferation was significantly higher in mutant cells as shown by the increased expression of Ki67, a protein expressed in all cycling/non-quiescent cells. Interestingly, when assessed by BrdU incorporation over a 5 day period, proliferation was found to be only increased in DN3 cells and wt in DN4 cells. Remarkably, the IL-2 receptor  $\alpha$ -chain CD25 was expressed at significantly higher levels by the mutant DN3 population (Fig.3C), a phenomenon observed in mice with defective pre-TCR signaling(27, 28). The expression of CD25 was similar to wt levels on peripheral cells. Finally, we were able to measure wt levels of intracellular TCR $\beta$  in mutant DN3 cells (Fig.3D) and only slightly reduced levels of extracellular TCR $\beta$  expression on mutant peripheral lymphocytes(Fig.3E). Taken together, our data indicate that the *memi* mutation dramatically impairs both pro- to pre-B- and DN3 to DN4 T-lymphocyte development in a manner similar to the *dCK<sup>-/-</sup>* knock-out model(18). This impairment is however incomplete, as some B- and T-cells are found in the periphery (Fig.1C).

### Splenomegaly and spleen composition in *dCK<sup>mem/mem</sup>* mice

In the periphery, we found that *dCK<sup>mem/mem</sup>* mice had much enlarged spleens (Fig.4A) with a significant increase in the absolute number of Ter119<sup>+</sup>-erythrocytes precursors and of myeloid cells (CD11b<sup>+</sup>, CD11c<sup>+</sup>, Gr1<sup>+</sup> or Ly-6A<sup>+</sup>) (Fig.4B). In the lymphocytic populations, CD4<sup>+</sup> T- and B220<sup>+</sup> B-cells were consistently decreased in numbers, whereas CD8<sup>+</sup> T-lymphocytes were present in absolute cell numbers equivalent to wt controls.

### Increased proliferation of *dCK<sup>mem/mem</sup>* peripheral T-lymphocytes

Our observation that LCMV-specific CD8<sup>+</sup> T-cells expressed high levels of KLRG1, a marker associated with replicative senescence (Fig.1B), prompted us to investigate the proliferative status of *dCK<sup>mem/mem</sup>* peripheral T-cells. BrdU incorporation was significantly increased in both mutant T-cell subpopulations(Fig.5A) and confirmed by the increased expression of Ki67 (Supp.Fig.3). *In vivo*, this increase correlated with a significantly higher ratio of cells with an effector memory phenotype: CD44<sup>high</sup>CD62L<sup>low</sup>(Fig.5B) and with

an increased level of activation (Supp.Fig.3) (29). This memory phenotype in the absence of antigen could imply a role for DCK in homeostatic proliferation.

To further confirm the change in proliferative status, splenocytes were analyzed *ex-vivo* for their cell-cycle progression pattern (Fig.5C). We observed a significant decrease in the G0/G1 population, correlating with a significant increase in S-phase cells (Supp.Fig.4). We investigated cell-cycle regulators in whole spleen extracts from *dCK<sup>mem/mem</sup>*, *dCK<sup>mem/+</sup>* and *dCK<sup>+/+</sup>* mice (Fig.5D). In *dCK<sup>mem/mem</sup>* cells, both cyclin D3 and cyclin A were expressed at higher levels than in wt controls, whereas p27Kip1 and pRb levels were decreased or undetectable. Protein extracts from lymph nodes confirmed those data. Finally, we found that the transcription factor Foxo3a was constitutively inactivated in *dCK<sup>mem/mem</sup>* splenocytes. These data indicate that the decreased quiescence observed in *dCK<sup>mem/mem</sup>* peripheral lymphocytes correlates with changes in the expression of cyclins and their co-regulators.

### Increased apoptosis of *dCK<sup>mem/mem</sup>* peripheral lymphocytes

The significant increase in proliferation observed in *dCK<sup>mem/mem</sup>* CD4<sup>+</sup> T-cell was not sufficient to restore absolute cell numbers equivalent to those found in wt controls, suggesting that survival might also be affected by the mutation. We therefore measured the population of Annexin V<sup>+</sup>/PI<sup>-</sup> lymphocytes and found that both CD4<sup>+</sup> and CD8<sup>+</sup> T-cells displayed a significant increase in apoptosis (Fig.5E). This correlated with an increase in the amount of active-caspase 3 (Supp.Fig.4), confirming that *memi* mutant T-cells undergo a higher rate of apoptotic cell-death in the periphery.

### *dCK<sup>mem/mem</sup>* increases proliferation and apoptosis in both a cell-intrinsic and - extrinsic manner

We next asked whether the proliferation, the cell-death or both resulted from a cell-intrinsic or -extrinsic effect of the mutation. To do so, we transferred either Thy1.1;*dCK<sup>+/+</sup>*CD4<sup>+</sup> T-cells into *Thy1.2;dCK<sup>mem/mem</sup>* recipients or *Thy1.2;dCK<sup>mem/mem</sup>*CD4<sup>+</sup> T-cells into Thy1.1;*dCK<sup>+/+</sup>* recipients (Fig.6A). At various time points, recipient blood was analyzed for the ratio of donor cells in the CD4<sup>+</sup> compartment. In *memi* hosts 6 days after injection onwards, we observed a significant augmentation in Thy1.1;*dCK<sup>+/+</sup>* donor cells ratio in the CD4<sup>+</sup> compartment (Fig.6B), suggesting an increase in wt donor cells proliferation. This increase in proliferation was confirmed when we measured Ki67 expression in splenic donor and endogenous cells 35 days after injection (Fig.6C). We indeed found that Ki67 expression was significantly higher in Thy1.1;*dCK<sup>+/+</sup>* donor cells in *memi* recipients than in Thy1.1;*dCK<sup>+/+</sup>* endogenous wt recipients cells.

In wt hosts, *Thy1.2;dCK<sup>mem/mem</sup>* donor cell ratios remained very low (Fig.6B), indicating that either *memi* cells have reverted to a quiescent naïve phenotype or that their level of proliferation is compensated by a high level of cell-death. Interestingly, the analysis of Ki67 expression in the splenocytes of wt recipients (Fig.6C) indicated that the level of proliferation in *Thy1.2;dCK<sup>mem/mem</sup>* donor cells was equivalent to the *Thy1.2;dCK<sup>mem/mem</sup>* endogenous cells in *memi* recipients and significantly higher than the Thy1.1;*dCK<sup>+/+</sup>* endogenous cells of the wt host. These data would indicate that even 35 days after transfer into a wt environment, the DCK-deficient *memi* cells are still highly proliferative. We therefore analyzed cell-death in the spleen of recipient mice 35d after injection (Fig.6D). We found that the level of apoptosis in Thy1.1;*dCK<sup>+/+</sup>* donor cells in *memi* recipient was significantly higher than in both *Thy1.2;dCK<sup>mem/mem</sup>* and Thy1.1;*dCK<sup>+/+</sup>* endogenous cells. As expected, the rate of apoptosis in *Thy1.2;dCK<sup>mem/mem</sup>* donor cells in wt recipients was high and equivalent to the one in *Thy1.2;dCK<sup>mem/mem</sup>* endogenous cells in the *memi* recipients.

The increased proliferation and maturation of wt CD4<sup>+</sup> T-cells in the *memi* host strongly supports a model of homeostatic proliferation in response to the lymphopenic DCK-deficient environment. This is accompanied by a high rate of apoptosis, as has been previously described for cells undergoing lymphopenia induced proliferation (LIP) (30, 31). Interestingly, the data obtained with *Thy1.2;dCK<sup>mem/mem</sup>* donor cells in wt recipients seemed to indicate that the absence of functional DCK could also control proliferation and cell-death in a cell-intrinsic manner. *memi*'s cell-intrinsic effect was further investigated in 1:1 chimera mice. Lethally irradiated wt recipient mice were injected with a 1:1 *Thy1.2;dCK<sup>mem/mem</sup>;Thy1.1;dCK<sup>+/+</sup>* mixture of BM cells depleted of their mature T-cells. Five weeks after the injection at least 95% of thymic and splenic cells were derived from wt progenitors, indicating that *memi* cells are outcompeted by wt cells during reconstitution (data not shown). In the thymus, the development of *Thy1.2;dCK<sup>mem/mem</sup>* thymocytes was impaired at the transition between DN3 and DN4 stages (Fig. 7A). In the periphery, both proliferation and apoptosis were significantly increased in *Thy1.2;dCK<sup>mem/mem</sup>* cells as compared to co-injected *Thy1.1;dCK<sup>+/+</sup>* controls (Fig. 7B). Altogether, these data indicate that *memi* impairs thymocytes development and induces excessive proliferation and apoptosis of peripheral T lymphocytes in a cell-intrinsic manner.

## Discussion

Our study describes a new point mutation in *dCK* and shows that it does not only impair lymphocyte development but also reduces quiescence and survival of peripheral hematopoietic cells. Our *dCK<sup>mem/mem</sup>* null mutation affects lymphocyte development in a manner similar to that reported for deletional deficiency in the *dCK<sup>-/-</sup>* knock-out mouse (18). The phenotypes of both *dCK<sup>-/-</sup>* and *dCK<sup>mem/mem</sup>* mice indicate that DCK is dispensable for non-hematopoietic developmental programs, but demonstrate an essential and non-redundant role for the protein in lymphopoiesis. In addition, our point mutation *memi* reveals an unexpected role for the nucleoside salvage pathway in the regulation of T-cell homeostatic proliferation and survival.

In the bone marrow, *memi* B-cell development is impaired at the transition between pro-B B220<sup>+</sup>CD43<sup>+</sup> and pre-B B220<sup>+</sup>CD43<sup>-</sup> cells. These are the stages at which immunoglobulin heavy V(D)J rearrangement takes place. In T-cells, V(D)J recombination and TCR $\beta$  rearrangement takes place at the DN3 stage. Cells with TCR  $\beta$  that cannot rearrange properly die of apoptosis. The TCR $\beta$  chain covalently couples to the pre-T $\alpha$  chain and CD3 to form the pre-TCR complex. In the absence of pre-TCR signaling, thymocytes development is severely affected at the DN3 to DN4 transition.

In their paper, Toy *et al.* propose two major hypotheses that could account for the T-lymphocyte development defects observed in *dCK<sup>-/-</sup>* mice. The first one would be that a deficiency in DCK and deoxynucleotide salvage impairs the considerable proliferation occurring at the DN3 stage, therefore reducing the DN4 population. However, in our hands with Ki67 expression, proliferation is significantly higher in mutant thymocytes (Fig. 3B). It therefore seems unlikely to us that impaired proliferation is the sole reason for the failings in lymphocytes development. The less pronounced increase in proliferation obtained with BrdU could be due to a high level of cell death in the mutant and the resulting loss of some BrdU<sup>+</sup> cells. Toy *et al.* also suggest that a defect in DCK could impair V(D)J recombination. In our mutant, we observe a significantly higher level of expression of the CD25/IL-2 receptor  $\alpha$ -chain in DN3 cells (Fig. 3C) as observed in cells from mice lacking pre-TCR signaling (27, 28). This could therefore indicate that a defect in dCK might impair TCR $\beta$  production or signaling. We were able to measure wt levels of intracellular TCR $\beta$  in mutant DN3 cells (Fig. 3D) supporting a normal V(D)J TCR $\beta$  recombination in DCK-deficient thymocytes and therefore pointing towards an impaired TCR signaling in DCK-deficient

cells. The phenotypes observed in *memi* mice are comparable to pre-T $\alpha$  deficient mice in which development is partially blocked between DN3 and DN4 stages and which present increased proliferation, apoptosis and memory cells in the periphery (32). Under ADA-deficient conditions, the accumulation of adenosine and deoxyadenosine has been shown to impair TCR signaling and directly induce apoptosis in developing thymocytes, respectively(33-35). As deoxyadenosine is one of DCK substrate, we could therefore hypothesize that a similar mechanism is operating in *memi* thymus whereby, in the absence of a functional DCK, deoxyadenosine and its derivatives accumulate and affect early thymocytes development through cell-intrinsic impairment of TCR signaling. However, even if severe, this developmental defect is only partial as some cells overcome the DCK deficiency, continue their development and migrate to the periphery. These cells might however represent a limited repertoire of specificity *i.e.*, they are oligoclonal populations expanded by homeostatic proliferation as exemplified with the CD8<sup>+</sup> T-cells response to LCMV (Fig.1A). Interestingly, the apparent absence of autoimmunity in this lymphopenic environment might be due to an increase in proportion of regulatory T-cells, a hypothesis that deserves further investigations.

In the periphery, two phenomena that have not been described before in a DCK-deficient context are observed: reduced quiescence and increased apoptosis.

Our transfers experiments (Fig.6) have shown that the proliferation is notably a cell-extrinsic effect of the *memi* mutation as wt cells injected into a *dCK<sup>mem/mem</sup>* host undergo proliferation. In a normal peripheral lymphocytic environment, mature T-cells remain quiescent for prolonged periods of time(4). This homeostatic survival relies on contact with self-peptide/MHC complex and IL-7. In an acute lymphopenic environment, these signals will become more available to the remaining naïve T-cells, resulting in LIP which restores almost normal levels of T-cells in the periphery. In animals chronically lymphopenic due to a complete or severe T-cell defect, like TCR<sup>-/-</sup> or animals with SCID, some transferred T-cells will adopt a form of rapid proliferation which is presumably driven by foreign antigens from commensal microflora(4). Finally, a third form of peripheral homeostatic proliferation has been observed when other  $\gamma$ -cytokines are present in excess and in which donor cells undergo a rapid proliferation (36, 37). In our immunodeficient *dCK<sup>mem/mem</sup>* mutants, we observe an important cell proliferation with an effector memory phenotype (CD44<sup>high</sup>CD62L<sup>low</sup>). A similar phenotype is found on wt cells transferred into a *memi* environment (Fig.6C and data not shown), clearly supporting a model of LIP. However, we also found that as late as 35 days after injection in wt hosts, *dCK<sup>mem/mem</sup>* cells still present a memory phenotype (CD44<sup>high</sup>CD62L<sup>low</sup>, data not shown), express high levels of Ki67 (Fig. 6C) and are apoptotic (Fig.6D). If the lymphocyte proliferation and subsequent apoptosis was exclusively driven by the *memi* lymphopenic environment, we would expect that once in a wt immunocompetent host, *dCK<sup>mem/mem</sup>* cells would revert to a more naïve quiescent phenotype. This is however not the case and the cell-intrinsic effect of *memi* on proliferation and cell-death was further supported by the data we obtained with 1:1 chimeric mice (Fig. 7B). The link between an impaired dCK pathway and the continuous inhibition of the Foxo3a pathway that we have observed in *memi* cells deserves further investigations.

The second phenomenon observed is a significant increase in apoptosis. Cells transferred into chronic lymphopenic recipients and undergoing LIP never really manage to reconstitute a normal lymphoid cellularity (38-42). Instead, the donor cells reach a plateau after a few weeks in the host and remain significantly proliferating and susceptible to Bim- and Fas-dependent cell-death (30, 31, 41). We therefore propose that the apoptosis observed in wt cells injected into chronically lymphopenic *memi* recipients is a direct consequence of LIP, whereas the increased apoptosis observed in *memi* cells is a cell-intrinsic effect of the mutation and could be a direct consequence of changes in their dNTP pools (43-46).



We have presented here a new null-mutant allele in the gene coding for deoxycytidine kinase, a crucial enzyme of the deoxynucleoside salvage pathway. The phenotypes described make a strong case for a vital non-redundant cell-intrinsic role for DCK during lymphocyte development. In addition, our study describes for the first time a crucial, non-redundant and cell-intrinsic role for DCK in peripheral homeostatic proliferation and survival. The data presented here support an effect of both the DCK-deficient environment and a cell-intrinsic effect of DCK deficiency on homeostatic proliferation. Our study might also have exposed a potential important regulator of hematopoietic quiescence in human and our mutant mouse might therefore be a valuable model of hematopoietic proliferative disorder in humans.

## Supplementary Material

Refer to Web version on PubMed Central for supplementary material.

## Acknowledgments

We thank M. Botto, F. Marelli-Berg, J. Dyson, E. Simpson and K. Hoebe for helpful discussions, K. Hoebe for the LOD score tools and L. Wang and the CBS for their technical support. We thank R. Welsh for the LCMV virus and L. P. Jordheim for the cell lines. O.C. and S.R. designed, performed experiments, analyzed data and co-wrote the manuscript; D.A.H, K.-K.H, P.J.M and H.G. performed experiments and analyzed data; E.W-F.L and P.G.A-R guided the experimental design.

## References

1. Tzachanis D, Lafuente EM, Li L, Boussiotis VA. Intrinsic and extrinsic regulation of T lymphocyte quiescence. *Leuk Lymphoma*. 2004; 45:1959–1967. [PubMed: 15370239]
2. Brumatti G, Salmanidis M, Ekert PG. Crossing paths: interactions between the cell death machinery and growth factor survival signals. *Cell Mol Life Sci*. 2010; 67:1619–1630. [PubMed: 20157838]
3. Skoda R. The genetic basis of myeloproliferative disorders. *Hematology Am Soc Hematol Educ Program*. 2007:1–10. [PubMed: 18024602]
4. Surh CD, Sprent J. Homeostasis of naive and memory T cells. *Immunity*. 2008; 29:848–862. [PubMed: 19100699]
5. Tothova Z, Gilliland DG. FoxO transcription factors and stem cell homeostasis: insights from the hematopoietic system. *Cell Stem Cell*. 2007; 1:140–152. [PubMed: 18371346]
6. Tefferi A, Gilliland DG. Oncogenes in myeloproliferative disorders. *Cell Cycle*. 2007; 6:550–566. [PubMed: 17351342]
7. Kaech SM, Wherry EJ, Ahmed R. Effector and memory T-cell differentiation: implications for vaccine development. *Nat Rev Immunol*. 2002; 2:251–262. [PubMed: 12001996]
8. Reichard P. Interactions between deoxyribonucleotide and DNA synthesis. *Annu Rev Biochem*. 1988; 57:349–374. [PubMed: 3052277]
9. Eriksson S, Munch-Petersen B, Johansson K, Eklund H. Structure and function of cellular deoxyribonucleoside kinases. *Cell Mol Life Sci*. 2002; 59:1327–1346. [PubMed: 12363036]
10. Nyhan WL. Disorders of purine and pyrimidine metabolism. *Mol Genet Metab*. 2005; 86:25–33. [PubMed: 16176880]
11. Giblett ER, Ammann AJ, Wara DW, Sandman R, Diamond LK. Nucleoside-phosphorylase deficiency in a child with severely defective T-cell immunity and normal B-cell immunity. *Lancet*. 1975; 1:1010–1013. [PubMed: 48676]
12. Giblett ER, Anderson JE, Cohen F, Pollara B, Meuwissen HJ. Adenosine-deaminase deficiency in two patients with severely impaired cellular immunity. *Lancet*. 1972; 2:1067–1069. [PubMed: 4117384]
13. Seegmiller JE, Rosenbloom FM, Kelley WN. Enzyme defect associated with a sex-linked human neurological disorder and excessive purine synthesis. *Science*. 1967; 155:1682–1684. [PubMed: 6020292]

14. Mandel H, Szargel R, Labay V, Elpeleg O, Saada A, Shalata A, Anbinder Y, Berkowitz D, Hartman C, Barak M, Eriksson S, Cohen N. The deoxyguanosine kinase gene is mutated in individuals with depleted hepatocerebral mitochondrial DNA. *Nat Genet.* 2001; 29:337–341. [PubMed: 11687800]
15. Saada A, Shaag A, Mandel H, Nevo Y, Eriksson S, Elpeleg O. Mutant mitochondrial thymidine kinase in mitochondrial DNA depletion myopathy. *Nat Genet.* 2001; 29:342–344. [PubMed: 11687801]
16. Zhou X, Solaroli N, Bjerke M, Stewart JB, Rozell B, Johansson M, Karlsson A. Progressive loss of mitochondrial DNA in thymidine kinase 2-deficient mice. *Hum Mol Genet.* 2008; 17:2329–2335. [PubMed: 18434326]
17. Dobrovolsky VN, Bucci T, Heflich RH, Desjardins J, Richardson FC. Mice deficient for cytosolic thymidine kinase gene develop fatal kidney disease. *Mol Genet Metab.* 2003; 78:1–10. [PubMed: 12559842]
18. Toy G, Austin WR, Liao HI, Cheng D, Singh A, Campbell DO, Ishikawa TO, Lehmann LW, Satyamurthy N, Phelps ME, Herschman HR, Czernin J, Witte ON, Radu CG. Requirement for deoxycytidine kinase in T and B lymphocyte development. *Proc Natl Acad Sci U S A.* 2010; 107:5551–5556. [PubMed: 20080663]
19. Arner ES, Eriksson S. Mammalian deoxyribonucleoside kinases. *Pharmacol Ther.* 1995; 67:155–186. [PubMed: 7494863]
20. Bergman AM, Pinedo HM, Peters GJ. Determinants of resistance to 2',2'-difluorodeoxycytidine (gemcitabine). *Drug Resist Updat.* 2002; 5:19–33. [PubMed: 12127861]
21. Lotfi K, Juliussen G, Albertioni F. Pharmacological basis for cladribine resistance. *Leuk Lymphoma.* 2003; 44:1705–1712. [PubMed: 14692522]
22. Du X, Tabeta K, Hoebe K, Liu H, Mann N, Mudd S, Crozat K, Sovath S, Gong X, Beutler B. Velvet, a dominant Egfr mutation that causes wavy hair and defective eyelid development in mice. *Genetics.* 2004; 166:331–340. [PubMed: 15020428]
23. Krol J, Francis RE, Albergaria A, Sunters A, Polychronis A, Coombes RC, Lam EW. The transcription factor FOXO3a is a crucial cellular target of gefitinib (Iressa) in breast cancer cells. *Mol Cancer Ther.* 2007; 6:3169–3179. [PubMed: 18089711]
24. Joshi NS, Cui W, Chandele A, Lee HK, Urso DR, Hagman J, Gapin L, Kaech SM. Inflammation directs memory precursor and short-lived effector CD8(+) T cell fates via the graded expression of T-bet transcription factor. *Immunity.* 2007; 27:281–295. [PubMed: 17723218]
25. Hoebe K, Jiang Z, Tabeta K, Du X, Georgel P, Crozat K, Beutler B. Genetic analysis of innate immunity. *Adv Immunol.* 2006; 91:175–226. [PubMed: 16938541]
26. Jordheim LP, Cros E, Gouy MH, Galmarini CM, Peyrottes S, Mackey J, Perigaud C, Dumontet C. Characterization of a gemcitabine-resistant murine leukemic cell line: reversion of in vitro resistance by a mononucleotide prodrug. *Clin Cancer Res.* 2004; 10:5614–5621. [PubMed: 15328204]
27. Laurent J, Bosco N, Marche PN, Ceredig R. New insights into the proliferation and differentiation of early mouse thymocytes. *Int Immunol.* 2004; 16:1069–1080. [PubMed: 15197172]
28. Mombaerts P, Iacomini J, Johnson RS, Herrup K, Tonegawa S, Papaioannou VE. RAG-1-deficient mice have no mature B and T lymphocytes. *Cell.* 1992; 68:869–877. [PubMed: 1547488]
29. Murali-Krishna K, Ahmed R. Cutting edge: naive T cells masquerading as memory cells. *J Immunol.* 2000; 165:1733–1737. [PubMed: 10925249]
30. Fortner KA, Bouillet P, Strasser A, Budd RC. Apoptosis regulators Fas and Bim synergistically control T-lymphocyte homeostatic proliferation. *Eur J Immunol.* 2010; 40:3043–3053. [PubMed: 21061436]
31. Fortner KA, Budd RC. The death receptor Fas (CD95/APO-1) mediates the deletion of T lymphocytes undergoing homeostatic proliferation. *J Immunol.* 2005; 175:4374–4382. [PubMed: 16177078]
32. Bosco N, Agenes F, Rolink AG, Ceredig R. Peripheral T cell lymphopenia and concomitant enrichment in naturally arising regulatory T cells: the case of the pre-Talpha gene-deleted mouse. *J Immunol.* 2006; 177:5014–5023. [PubMed: 17015684]

33. Apasov SG, Blackburn MR, Kellems RE, Smith PT, Sitkovsky MV. Adenosine deaminase deficiency increases thymic apoptosis and causes defective T cell receptor signaling. *J Clin Invest.* 2001; 108:131–141. [PubMed: 11435465]
34. Huang S, Apasov S, Koshiba M, Sitkovsky M. Role of A2a extracellular adenosine receptor-mediated signaling in adenosine-mediated inhibition of T-cell activation and expansion. *Blood.* 1997; 90:1600–1610. [PubMed: 9269779]
35. Lappas CM, Rieger JM, Linden J. A2A adenosine receptor induction inhibits IFN-gamma production in murine CD4+ T cells. *J Immunol.* 2005; 174:1073–1080. [PubMed: 15634932]
36. Cho JH, Boyman O, Kim HO, Hahm B, Rubinstein MP, Ramsey C, Kim DM, Surh CD, Sprent J. An intense form of homeostatic proliferation of naive CD8+ cells driven by IL-2. *J Exp Med.* 2007; 204:1787–1801. [PubMed: 17664294]
37. Ramsey C, Rubinstein MP, Kim DM, Cho JH, Sprent J, Surh CD. The lymphopenic environment of CD132 (common gamma-chain)-deficient hosts elicits rapid homeostatic proliferation of naive T cells via IL-15. *J Immunol.* 2008; 180:5320–5326. [PubMed: 18390713]
38. Murali-Krishna K, Lau LL, Sambhara S, Lemonnier F, Altman J, Ahmed R. Persistence of memory CD8 T cells in MHC class I-deficient mice. *Science.* 1999; 286:1377–1381. [PubMed: 10558996]
39. Cho BK, Rao VP, Ge Q, Eisen HN, Chen J. Homeostasis-stimulated proliferation drives naive T cells to differentiate directly into memory T cells. *J Exp Med.* 2000; 192:549–556. [PubMed: 10952724]
40. Ge Q, Rao VP, Cho BK, Eisen HN, Chen J. Dependence of lymphopenia-induced T cell proliferation on the abundance of peptide/ MHC epitopes and strength of their interaction with T cell receptors. *Proc Natl Acad Sci U S A.* 2001; 98:1728–1733. [PubMed: 11172019]
41. Goldrath AW, Bogatzki LY, Bevan MJ. Naive T cells transiently acquire a memory-like phenotype during homeostasis-driven proliferation. *J Exp Med.* 2000; 192:557–564. [PubMed: 10952725]
42. Tanchot C, Le Champion A, Martin B, Leament S, Dautigny N, Lucas B. Conversion of naive T cells to a memory-like phenotype in lymphopenic hosts is not related to a homeostatic mechanism that fills the peripheral naive T cell pool. *J Immunol.* 2002; 168:5042–5046. [PubMed: 11994456]
43. Bradley MO, Sharkey NA. Mutagenicity of thymidine to cultured Chinese hamster cells. *Nature.* 1978; 274:607–608. [PubMed: 566859]
44. Brox L, Ng A, Pollock E, Belch A. DNA strand breaks induced in human T-lymphocytes by the combination of deoxyadenosine and deoxycoformycin. *Cancer Res.* 1984; 44:934–937. [PubMed: 6607110]
45. Mathews CK, Ji J. DNA precursor asymmetries, replication fidelity, and variable genome evolution. *Bioessays.* 1992; 14:295–301. [PubMed: 1637360]
46. Oliver FJ, Collins MK, Lopez-Rivas A. dNTP pools imbalance as a signal to initiate apoptosis. *Experientia.* 1996; 52:995–1000. [PubMed: 8917730]

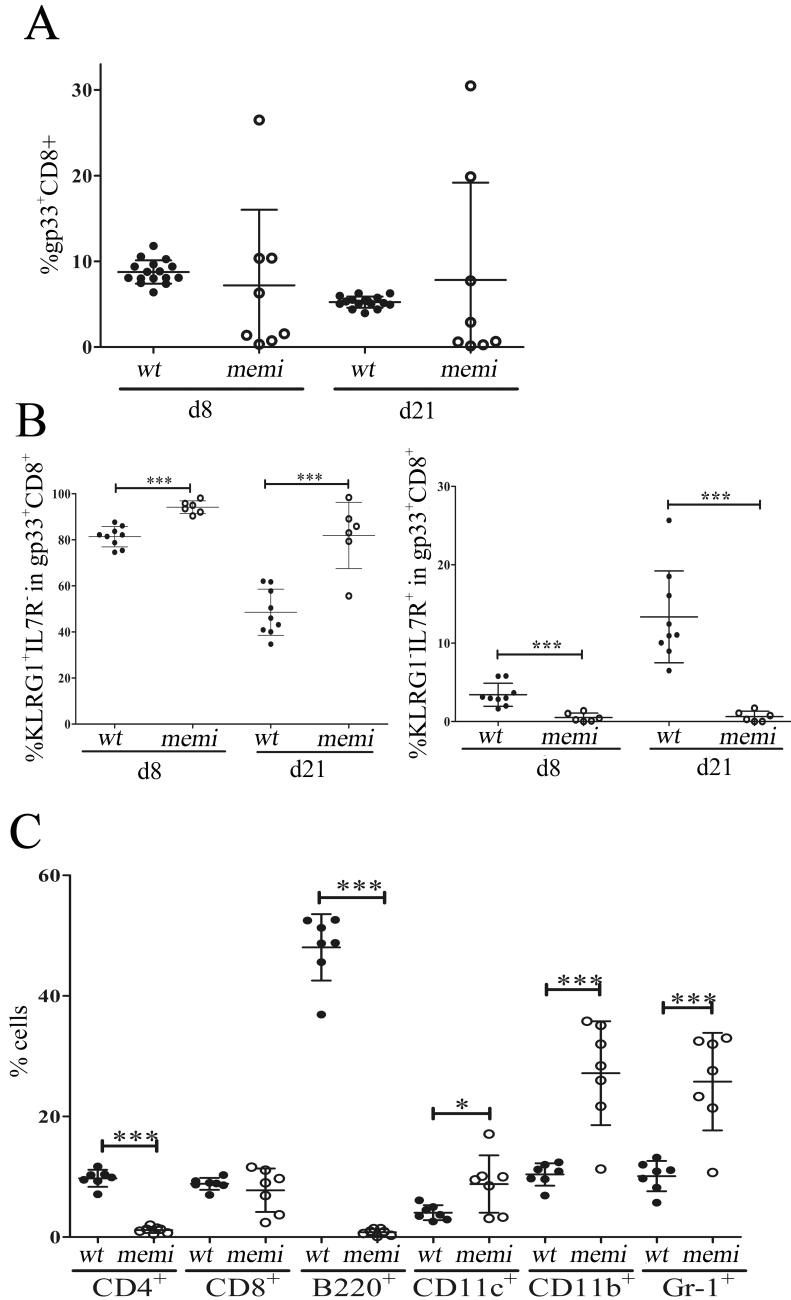


**Figure 1. *memi* mice present a distinctive immune response upon LCMV infection and a mutant peripheral blood composition in naïve conditions**

(A) Six-week old wt and *memi* mice were injected with LCMV Armstrong and their antigen-specific CD8<sup>+</sup> T-cells (gp33<sup>+</sup>CD8<sup>+</sup>) measured at d8 and d21 after infection. The graph is representative of at least 12 independent experiments. Here, n = 18 for wt and 9 for *memi*.

(B) Wt and *memi* mice were injected with LCMV Armstrong and their effector (KLRG1<sup>+</sup>IL-7R<sup>-</sup>gp33<sup>+</sup>CD8<sup>+</sup>, left graph) and memory precursors (KLRG1<sup>-</sup>IL-7R<sup>+</sup>gp33<sup>+</sup>CD8<sup>+</sup>, right graph) T-cells measured 8 and 21 d after infection. The graphs are representative of at least 12 independent experiments. Here, n = 9 for wt and 6 for *memi*.

*memi*. In all experiments, error bars represent standard deviation and \* $p < 0.05$ , \*\* $p < 0.01$ , \*\*\* $p < 0.001$ .

(C) Peripheral blood was stained with specific antibodies against lymphocytes and myeloid cells and analyzed by flow cytometry. These data are representative of 5 independent experiments. Here,  $n = 7$  for wt and *memi*.

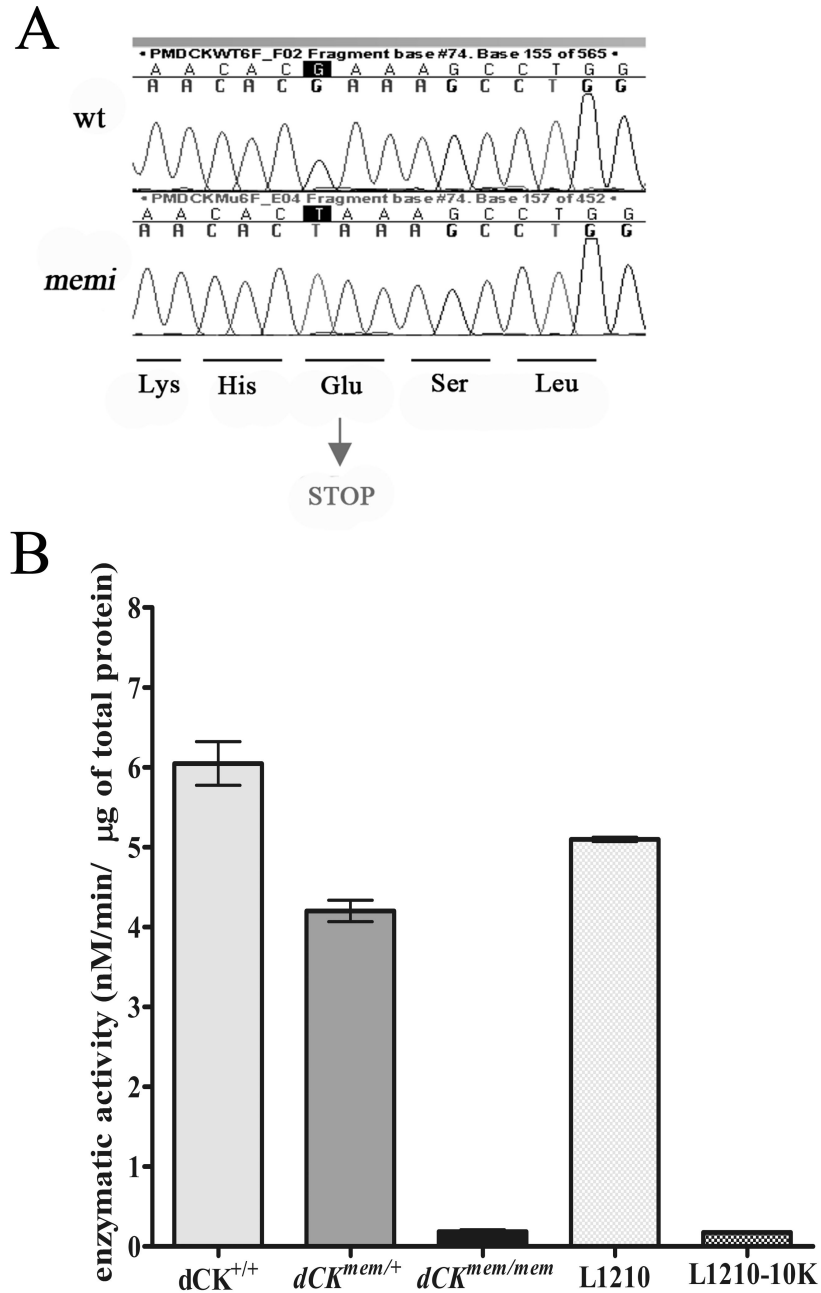


**Figure 2. *memi* is a null point mutation in *dCK***

(A) The *memi* mutation is a single nucleotide transversion (G to T) at nucleotide 739 in exon 6 of *dCK*. This modification changes the glutamic acid (Glu) 247 into an early translational terminating codon (STOP).

(B) *In vitro* DCK enzymatic activity assay was performed using cell lysates from *dCK*<sup>*mem*/*mem*</sup>, *dCK*<sup>*mem*/+</sup> and *dCK*<sup>+/+</sup> spleens. L1210 and L1210-10K cell-lines were used as positive and negative controls(26). The graph is representative of 2 independent experiments in which DCK activity was analyzed in triplicate with samples pooled from 3 mice per genotype.

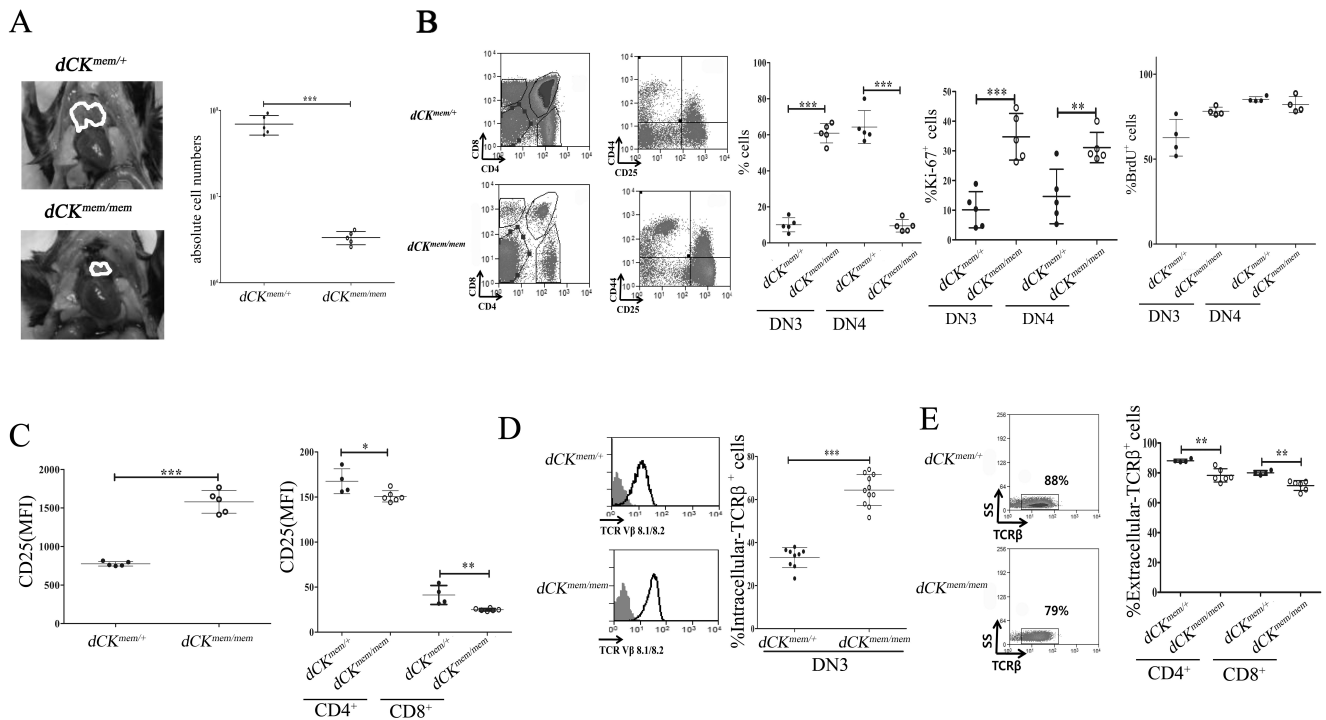


**Figure 3. *dCK<sup>mem/mem</sup>* mice have profound defects in lymphocyte development**

(A) *dCK<sup>mem/mem</sup>* mice have reduced thymic size and cellularity. Thymi of two representative mice are indicated by the white lines. The graph is representative of 4 independent experiments, n 3.

(B) *dCK<sup>mem/mem</sup>* T-cells development is blocked at the transition between the DN3 and DN4 stages. The dot plots are from 2 representative mice, the graph representative of 3 independent experiments, n=5. Proliferation of mutant DN3 and DN4 cells was assessed by measuring Ki67 expression (middle graph) or BrdU incorporation (right graph). The graphs are representative of 2 independent experiments, n 4.

(C): The mean fluorescence intensity (MFI) obtained for CD25 expression in the DN3 population (left panel) and in peripheral cells (right panel) is indicated. These data are representative of 3 independent experiments, n 4.

(D) Expression of intracellular TCR- $\text{V}\beta 8.1/8.2$  in DN3 thymocytes. The histograms are of 2 representative mice with TCR $\beta$ -negative DN1 control (grey) and DN3 cells (black). The graph is representative of 2 independent experiments, n 4.

(E) Surface expression of TCR $\beta$  on peripheral T-lymphocytes. The histograms are of 2 representative mice and the data representative of 2 independent experiments, n 4.

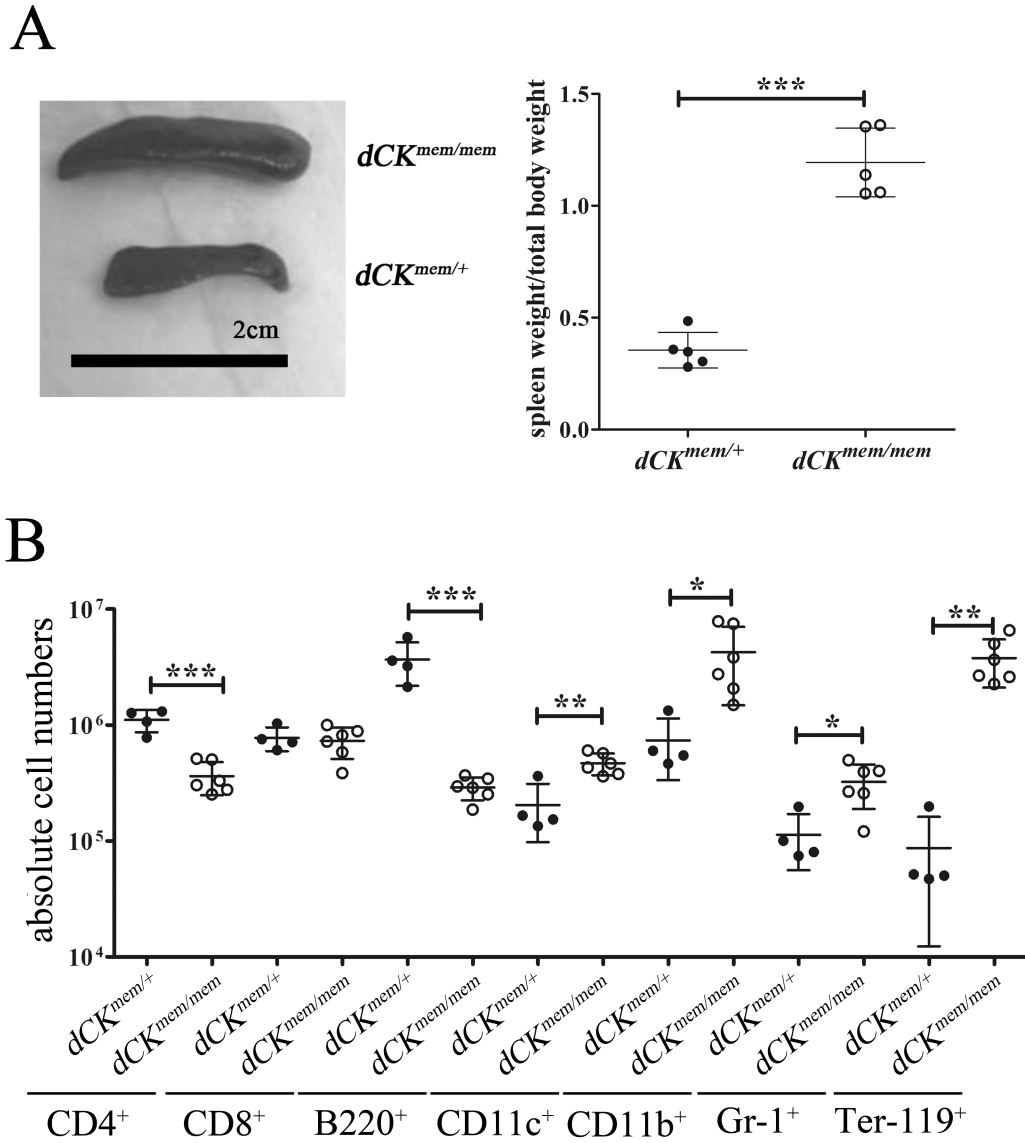


**Figure 4.  $dCK^{mem/mem}$  mice present an important splenomegaly due to an increase in non-lymphoid cells**

(A) Splens from 2 representative  $dCK^{mem/mem}$  and  $dCK^{mem/+}$  mice. The relative spleen weights were obtained by dividing individual spleen weights by the corresponding total body weight,  $n=5$ .

(B) Spleen composition in  $dCK^{mem/mem}$  and  $dCK^{mem/+}$  mice. This graph is representative of 3 independent experiments,  $n=3$ . Similar data have been obtained for B cells with a CD19 specific antibody.



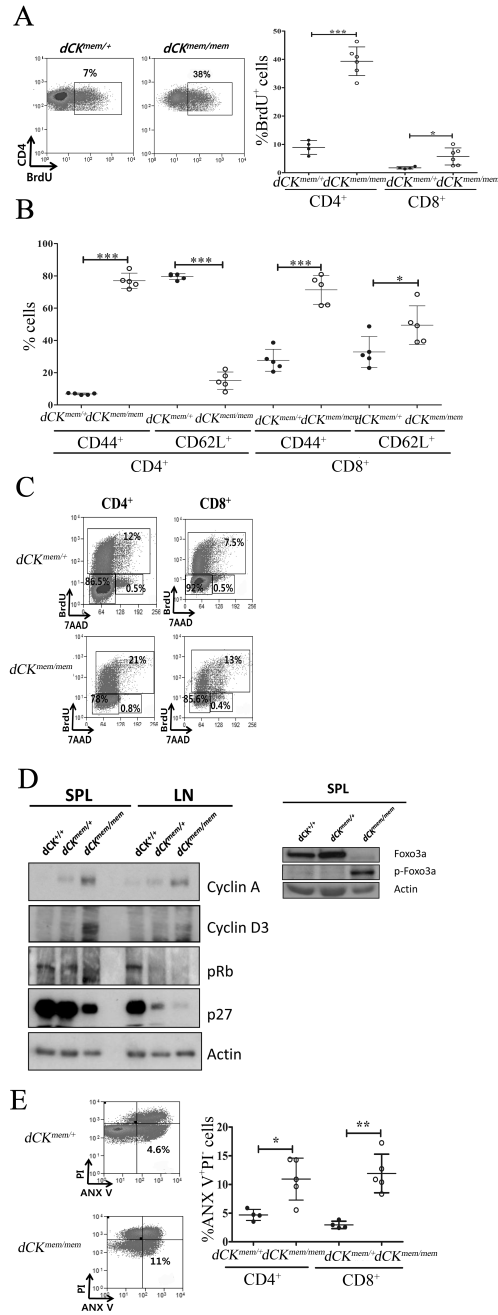


**Figure 5. *dCK<sup>mem/mem</sup>* splenocytes are hyper-proliferative and apoptotic**  
 (A) Mutant CD4<sup>+</sup> and CD8<sup>+</sup> T-cells are significantly hyper-proliferative as indicated by BrdU incorporation. The histograms are of 2 representative mice and the graph representative of 3 independent experiments, n = 3.  
 (B) Expression of CD44 and CD62L on mutant and wt peripheral blood T-cells. These data are representative of 3 independent experiments, n = 3.  
 (C) Cell-cycle analysis of T-lymphocytes using a BrdU/7-AAD staining. The histograms are of 2 representative mice from 3 independent experiments.  
 (D) Western blots for Cyclin A, Cyclin D3, pRb, p27, and Actin in SPL and LN.  
 (E) ANX V staining and %ANX V PI<sup>+</sup> cells.

(D) Expression pattern of cell-cycle regulators in *dCK<sup>mem/mem</sup>* mice. Western blot analysis was done with samples from spleen (SPL) or inguinal lymph nodes (LN). The experiment was done twice independently with pooled samples of 3 mice per genotype and per organ. (E) Apoptotic CD4<sup>+</sup> and CD8<sup>+</sup> T-cells were detected in the AnnexinV<sup>+</sup>/PI<sup>-</sup> quadrant. The histograms are from 2 representative mice and the graph representative of 2 independent experiments, n 4.

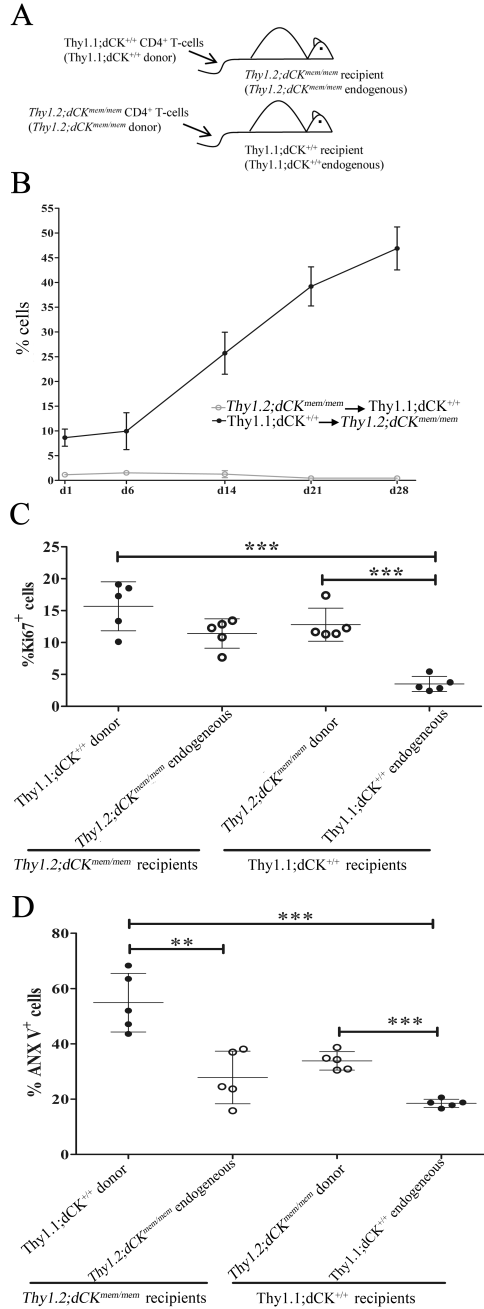


**Figure 6. proliferation and apoptosis are controlled by both cell-extrinsic and -intrinsic mechanisms**

(A) Thy1.1;dCK<sup>+/+</sup> CD4<sup>+</sup> T-cells were transferred into non-irradiated *Thy1.2;dCK<sup>mem/mem</sup>* recipients and *Thy1.2;dCK<sup>mem/mem</sup>* CD4<sup>+</sup> T-cells into non-irradiated Thy1.1;dCK<sup>+/+</sup> hosts. All the panels are representative of 2 independent experiments with 5 recipients per group. (B) The percentage of Thy1.1;dCK<sup>+/+</sup> donor cells in the *memi* recipient CD4<sup>+</sup> compartment (black line) and of *Thy1.2;dCK<sup>mem/mem</sup>* donor cells in the wt recipient CD4<sup>+</sup> compartment (grey line) is represented.

(C) The proliferation of donor and endogenous cells was measured by Ki-67 expression in recipients' splenocytes 35 days after transfer.

(D) Apoptosis of donor and endogenous cells was measured in recipients' splenocytes 35 days after transfer.

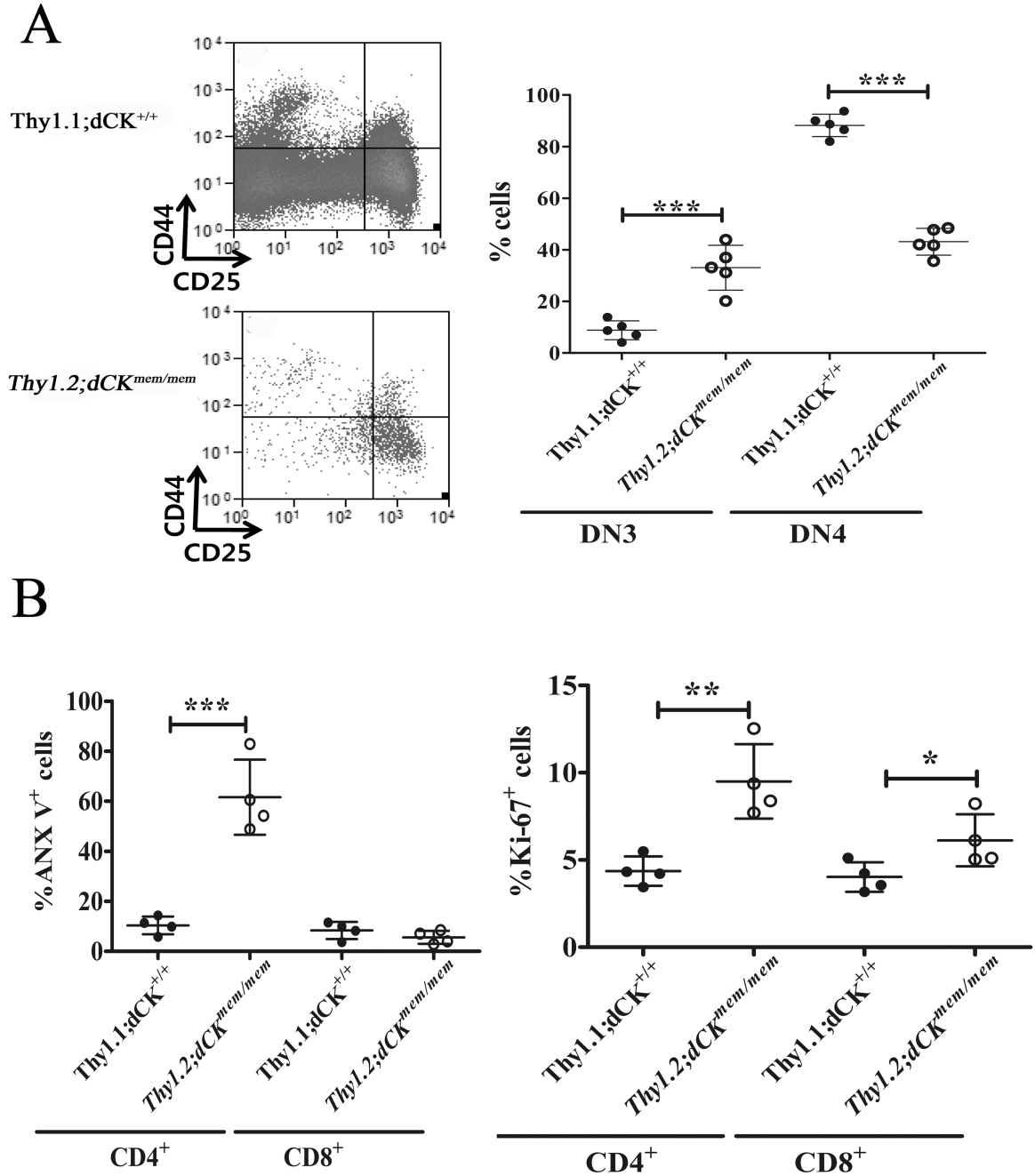


**Figure 7. *memi* acts on thymocytes' development and peripheral lymphocytes' proliferation and apoptosis in a cell-intrinsic manner**

Lethally irradiated wt recipient mice were injected with a 1:1

*Thy1.2; dCK<sup>mem/mem</sup>; Thy1.1; dCK<sup>+/+</sup>* mixture of BM cells depleted of their mature T-cells.

The recipient mice were analyzed 5 weeks after the injection.

(A): By gating on either *Thy1.1*<sup>+</sup> wt or *Thy1.2*<sup>+</sup> *memi* cells, thymocytes were analyzed in the recipient mice for their DN cells distribution. The histograms are from 2 representative mice and the graph from 2 independent experiments, n = 4.

(B): Apoptosis and proliferation were analyzed by gating splenic lymphocytes for either Thy1.1<sup>+</sup> wt or Thy1.2<sup>+</sup> *mem* populations and measuring annexinV or Ki67 expression, respectively. The graphs are representative of 2 independent experiments, n = 4.